

Theoretical studies of electronic properties of semimagnetic superlattices in a magnetic field

G. Y. Wu and T. C. McGill

California Institute of Technology, Pasadena, California 91125

D. L. Smith

Los Alamos National Laboratory, Los Alamos, New Mexico 87545

C. Mailhot

Xerox Webster Research Center, Webster, New York 14580

(Received 15 December 1986; accepted 7 April 1987)

We present our first theoretical study of the electronic properties of superlattices formed from semimagnetic semiconductors. Both $\text{Cd}_{0.8}\text{Mn}_{0.2}\text{Te}/\text{Cd}_{0.7}\text{Mn}_{0.3}\text{Te}$ and $\text{Hg}_{0.95}\text{Mn}_{0.05}\text{Te}/\text{Cd}_{0.78}\text{Mn}_{0.22}\text{Te}$ systems are considered explicitly. Magnetic field splittings are calculated with and without the exchange interaction. We find that the exchange interaction dominates the magnetic effects in the wide-gap $\text{Cd}_{0.8}\text{Mn}_{0.2}\text{Te}/\text{Cd}_{0.7}\text{Mn}_{0.3}\text{Te}$ system while the Landau level shift is also important in the $\text{Hg}_{0.95}\text{Mn}_{0.05}\text{Te}/\text{Cd}_{0.78}\text{Mn}_{0.22}\text{Te}$ system. We present calculations of the superlattice band-gap variation with temperature and its derivative with magnetic field as a function of the superlattice layer thickness. Variation of the band offset in determining the values of the various quantities is examined.

I. INTRODUCTION

The growth of high-quality $\text{Cd}_{1-x}\text{Mn}_x\text{Te}/\text{Cd}_{1-y}\text{Mn}_y\text{Te}$ superlattices and $\text{Hg}_{1-x}\text{Mn}_x\text{Te}$ epilayers has recently been demonstrated using molecular-beam epitaxy techniques.¹⁻⁵ Growth has been achieved with both a [111] and [100] growth axis.⁶ These materials are particularly interesting because of the presence of the magnetic Mn^{++} ion. The strong exchange interaction between the localized 3d electrons of the Mn^{++} ions and itinerant band electrons give rise to large Zeeman splittings of the energy bands. Magneto-optic studies of these superlattice systems have recently been performed.⁷⁻⁹ Magnetic field dependence of the luminescence has been seen. Laser emission has been observed from these superlattices.¹⁰ The energy of the stimulated emission peak has been shifted by application of a magnetic field.

In this paper, we report our first theoretical study of the electronic properties of semimagnetic superlattices in a magnetic field. We consider superlattices made from layers of $\text{Cd}_{1-x}\text{Mn}_x\text{Te}$ and $\text{Hg}_{1-y}\text{Mn}_y\text{Te}$ with different alloy compositions. In Sec. II, we present the method used to calculate the properties of the superlattices. In Sec. III, we present the results for $\text{Cd}_{1-x}\text{Mn}_x\text{Te}$ superlattices formed by layering materials with different values of x . In Sec. IV, we present the results for $\text{Hg}_{1-y}\text{Mn}_y\text{Te}/\text{Cd}_{1-x}\text{Mn}_x\text{Te}$ superlattices. In Sec. V, we conclude and summarize our study.

II. THEORETICAL METHOD

Our theoretical calculations are based upon Ref. 11 modified to include the effects of magnetic fields and the exchange interaction in mean-field theory using the virtual-crystal approximation.^{12,13} A theoretical paper will be published describing the k.p theory of a superlattice under the influence of a magnetic field. Parameters describing the average spin state of the Mn^{++} ions as a function of magnetic field and temperature are taken from Refs. 14 and 15. The values of

the exchange matrix elements are also from Refs. 14 and 15. We assume that these matrix elements and spin parameters are the same in the layers forming the superlattice as they are in the corresponding bulk alloys. We specifically study $\text{Cd}_{0.8}\text{Mn}_{0.2}\text{Te}/\text{Cd}_{0.7}\text{Mn}_{0.3}\text{Te}$ with a wide band gap and $\text{Hg}_{0.95}\text{Mn}_{0.05}\text{Te}/\text{Cd}_{0.78}\text{Mn}_{0.22}\text{Te}$ with a narrow band gap. For the $\text{Cd}_{0.8}\text{Mn}_{0.2}\text{Te}/\text{Cd}_{0.7}\text{Mn}_{0.3}\text{Te}$ system, the small lattice constant difference ($\approx 0.25\%$) between the two constituent materials is neglected. The valence-band offset is taken to be zero since the band-gap difference is believed to occur primarily in the conduction band.^{8,9} The $X = 0.2$ alloy has the smaller band gap and is therefore the quantum well material for electrons. Momentum matrix elements and the spin-orbit interaction parameter are taken to be the same in the two constituents and to be equal to those of CdTe given in Ref. 16. The band gaps of the constituent materials are from Refs. 17 and 18. For the $\text{Hg}_{0.95}\text{Mn}_{0.05}\text{Te}/\text{Cd}_{0.78}\text{Mn}_{0.22}\text{Te}$ system, the Mn^{++} composition is chosen in such a way that the strain is zero.¹⁸ We consider materials with a [100] growth axis. The magnetic field is taken to be parallel to the growth axis.

For bulk zinc-blende semiconductors with a uniform magnetic field in the Z direction and a gauge choice so that the vector potential is in the X direction, quantum numbers include the wave vectors k_x , k_z and a Landau level index N . The zeroth-order wave functions have the form

$$\Psi(\mathbf{r}) = e^{i(k_x X + k_z Z)} \sum_d C_d h_{n(d,N)}(y') U_d(\mathbf{r}),$$

where

$$y' = y - (\hbar c k_x / e B). \quad (1)$$

Here C_d is an expansion coefficient, h_n is a harmonic oscillator eigenfunction, U_d is a periodic Kramer basis function, d labels these basis functions, and the index of the harmonic oscillator eigenfunction n depends on both the quantum

number N and the basis function d . For a superlattice with B parallel to the growth axis, k_x and N together with a superlattice wave vector Q_z are good quantum numbers. That is, the superlattice wave function is made of a coherent sum of states like that of Eq. (1) in each material. All states in the sum have the same energy, k_x and N ; the sum is over k_z which may be complex. Imposing boundary conditions at the superlattice interfaces and considering the superlattice translational symmetry in the Z direction gives an eigenvalue equation from which one determines the superlattice wave functions and dispersion relations. Within mean-field theory and virtual-crystal approximation, the exchange term in the Hamiltonian is

$$H_x = X_{Mn} \sum_j J(\mathbf{r} - \mathbf{R}_j) \langle S_z \rangle \sigma_z, \quad (2)$$

where j is a cation site. The exchange interaction greatly increases the size of the spin splittings produced by the magnetic field, but it does not change the symmetry of the problem.

III. SUPERLATTICES OF $\text{Cd}_{1-x}\text{Mn}_x\text{Te}$

In Fig. 1, we show the lowest conduction-band and highest valence-band energy levels at $Q_z = 0$ for a $\text{Cd}_{0.8}\text{Mn}_{0.2}\text{Te}/\text{Cd}_{0.7}\text{Mn}_{0.3}\text{Te}$ superlattice consisting of six

molecular layers of each constituent material for three cases: no magnetic field, a magnetic field of 5 T neglecting exchange interaction (at high spin temperature), and a magnetic field of 5 T including the exchange interaction (at zero spin temperature¹⁹). At $B = 0$, the conduction-band states are twofold degenerate and the valence-band states are fourfold degenerate. (Because the valence-band offset is taken to be zero and lattice mismatch is neglected, there is no splitting of the heavy- and light-hole bands.) For the $B = 5$ T and high spin temperature case, all degeneracies are broken, the conduction-band states move to higher energy and the valence-band states to lower energy. However, the size of the splittings and the motion of the levels are quite small. (The splittings of the two conduction-band states and the highest two valence-band states are so small that they are not resolved in Fig. 1.) For the $B = 5$ T and zero temperature case, much larger splittings, due to the exchange interaction, occur and the band gap of the superlattice is decreased by the magnetic field. The state labeling follows that of Ref. 20. (In principle, states corresponding to the "a" and "b" labeling of Ref. 20 are mixed and the more complete labeling scheme described above should be used. However, the mixing is small and the simpler scheme of Ref. 20 is used in Fig. 1.) All states shown are made up primarily of $n = 0$ harmonic oscillator eigenfunctions. The state labeled $a(0)$ has primarily $|S = 1/2\rangle$ atomic character, $b(0)$ has primarily $|S = -1/2\rangle$

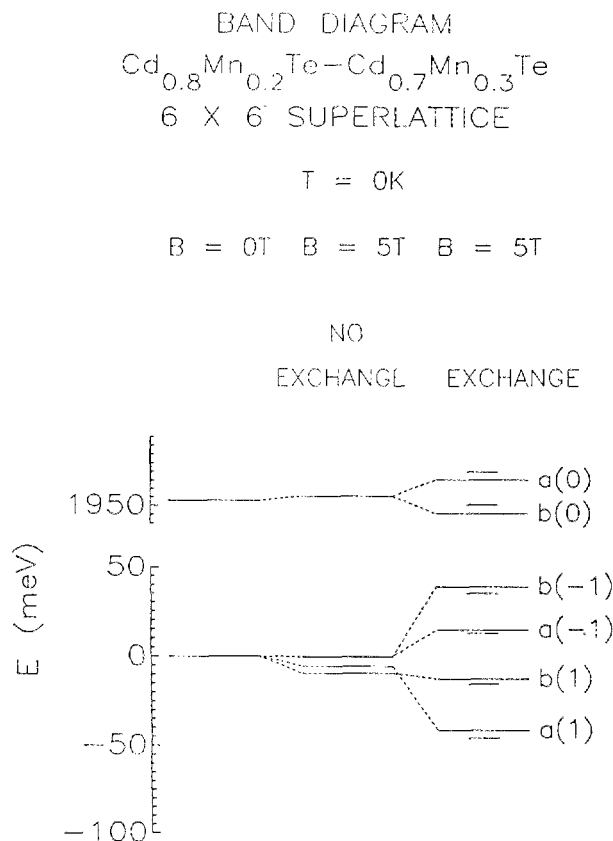


FIG. 1. Energy levels of the lowest conduction-band and highest valence-band states at $Q_z = 0$ for a $\text{Cd}_{0.8}\text{Mn}_{0.2}\text{Te}/\text{Cd}_{0.7}\text{Mn}_{0.3}\text{Te}$ superlattice consisting of six molecular layers of each constituent material for three cases: no magnetic field, a magnetic field of 5 T neglecting exchange interaction, and a magnetic field of 5 T including the exchange interaction.

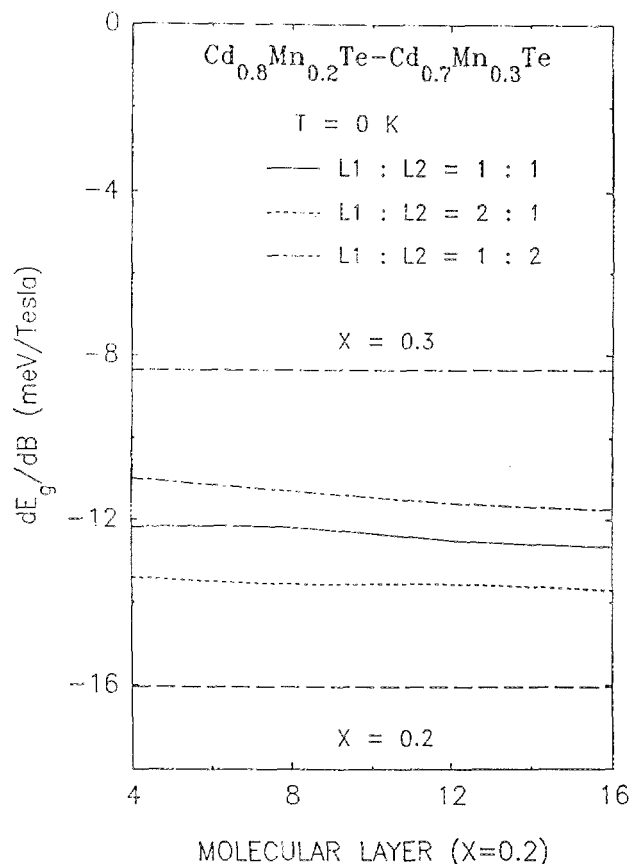


FIG. 2. The derivative of the $\text{Cd}_{0.8}\text{Mn}_{0.2}\text{Te}/\text{Cd}_{0.7}\text{Mn}_{0.3}\text{Te}$ superlattice band gap with magnetic field as a function of the $X = 0.2$ alloy layer thickness for three layer thickness ratios. The corresponding derivatives for the $X = 0.2$ and 0.3 alloys are shown as straight lines.

character, $b(-1)$ has primarily $|3/2 - 3/2\rangle$ character, $a(-1)$ has primarily $|3/2 - 1/2\rangle$ character, $b(1)$ has primarily $|3/2 1/2\rangle$ character, and $a(1)$ has primarily $|3/2 3/2\rangle$ character. The unlabeled lines indicate the energy levels of states made up primarily from $n = 1$ harmonic oscillator functions. The positions of states made primarily from higher harmonic oscillator functions are not shown. It is clear from Fig. 1 that the magnetic field splittings in the superlattice are dominated by the exchange interaction. The relative change in the band gap is $\approx 2.5\%$.

In Fig. 2, the derivative of the band gap with magnetic field of the $\text{Cd}_{0.8}\text{Mn}_{0.2}\text{Te}/\text{Cd}_{0.7}\text{Mn}_{0.3}\text{Te}$ superlattice at small magnetic field and zero temperature¹⁹ is shown as a function of the number of molecular layers of the $X = 0.2$ alloy for three ratios of the superlattice layer thicknesses. Also shown, for comparison, are the corresponding derivatives for the two constituent alloys. First, notice that the derivative of the $X = 0.3$ alloy is less than that of the $X = 0.2$ alloy. This occurs, according to the results of Ref. 14, because of stronger antiferromagnetic coupling in the $X = 0.3$ alloy. That is, the net Mn^{++} spin (absolute value of the composition times the average spin $X\langle S_z \rangle$) is larger in the $X = 0.2$ alloy than in the $X = 0.3$ alloy at zero temperature and small magnetic fields. The derivatives in the superlattice lie between those of the alloys. For the thin layer superlattices, the results are simply averaged. That is, the 1:1 superlattice result is halfway between the $X = 0.2$ and 0.3 alloys; the 2:1 superlattice is $\frac{1}{3}$ and the 1:2 superlattice is $\frac{2}{3}$ of the way between the $X = 0.2$ and 0.3 alloys. For thin superlattices, the electron and hole wave functions are not well confined by energy barriers. Indeed, the only barrier for holes is due to the exchange interaction itself, like the "spin superlattices" of Ref. 21. As the superlattice layer thicknesses increase, the magnitude of the derivative increases, moving toward the value of the $X = 0.2$ alloy. This occurs because the carrier wave functions are better confined in the $X = 0.2$ alloy in the thicker superlattices. The effect is not very large, however, because the barrier for holes is small and the exchange interaction is larger for holes than for the electrons.

In Fig. 3, we show the change in band gap with magnetic field at three magnetic fields for a $\text{Cd}_{0.8}\text{Mn}_{0.2}\text{Te}/\text{Cd}_{0.7}\text{Mn}_{0.3}\text{Te}$ superlattice consisting of eight molecular layers of each alloy as a function of inverse temperature.¹⁹ The arrows indicate the zero temperature asymptotes. The band-gap reduction is due to the exchange interaction of the band electrons with localized $3d$ electrons on Mn^{++} . At low temperatures the Mn^{++} spins align in the direction opposite to the magnetic field leading to a net interaction with the band electrons. At higher temperatures, the Mn^{++} spins are randomized and there is no net exchange interaction with band electrons (within mean field theory). From the figure, one sees that the strength of the net exchange interactions decreases rapidly with increasing temperature for temperatures above 5 K.

IV. SUPERLATTICES OF $\text{Hg}_{1-y}\text{Mn}_y\text{Te}/\text{Cd}_{1-x}\text{Mn}_x\text{Te}$

In Fig. 4, we show the energy levels at $Q_z = 0$ for a $\text{Hg}_{0.95}\text{Mn}_{0.05}\text{Te}/\text{Cd}_{0.78}\text{Mn}_{0.22}\text{Te}$ superlattice consisting of 15 molecular layers of each constituent material.¹⁹ The va-

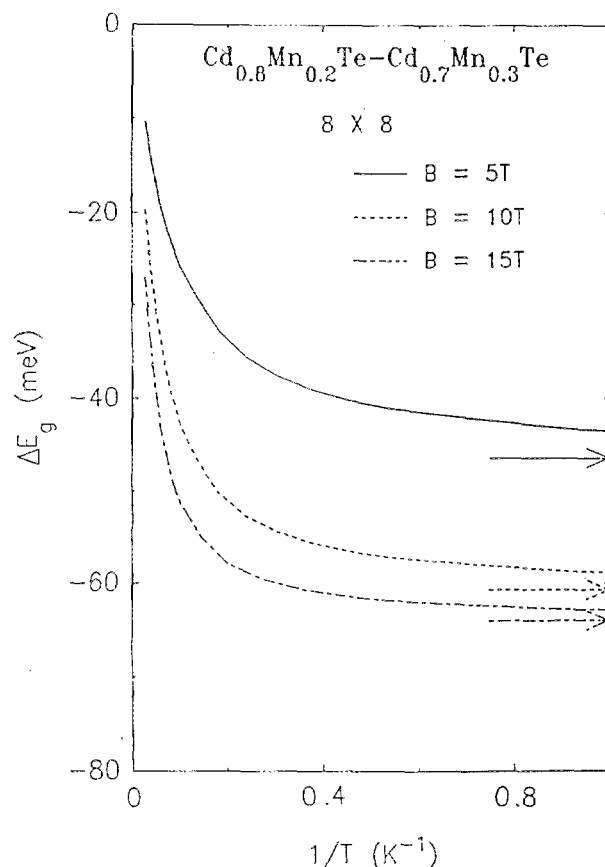


FIG. 3. Change in band gap of the 8×8 $\text{Cd}_{0.8}\text{Mn}_{0.2}\text{Te}/\text{Cd}_{0.7}\text{Mn}_{0.3}\text{Te}$ superlattice as a function of inverse temperature and three magnetic fields. Arrows indicate the zero temperature asymptotes.

lence-band offset is taken to be zero tentatively. The dependence of magnetic effects on the value of valence-band offset is shown in later figures. At $B = 0$, the conduction-band states are twofold degenerate and the valence-band states are fourfold degenerate due to choices of zero valence-band offset and zero strain. For the $B = 5$ T and high spin temperature case, all degeneracies are broken, the conduction-band states move to higher energy and the valence-band states to lower energy. For the $B = 5$ T and zero spin temperature case, much larger splittings, due to the exchange interaction, occur and the band gap of the superlattice is decreased by the magnetic field. The states are labeled according to the primary wave function characters they carry. We note that the conduction-band states with a strong $|3/2 1/2\rangle$ ($|3/2 - 1/2\rangle$) character also carry a $|S 1/2\rangle$ ($|S - 1/2\rangle$) character of comparable magnitude. However, the exchange integrals for light-hole and S characters have opposite signs with the exchange integral for the light-hole states being larger in magnitude than that for the S states.¹⁵ Since order of the splitting is determined by the light-hole character, we label the conduction-band states showing only their light-hole character. We find that the Landau level shift of the conduction-band states is larger than that in $\text{Cd}_{0.8}\text{Mn}_{0.2}\text{Te}/\text{Cd}_{0.7}\text{Mn}_{0.3}\text{Te}$ since the lighter electron effective mass here gives rise to a larger cyclotron frequency which, in turn, induces a larger Landau level shift. The splittings of valence-

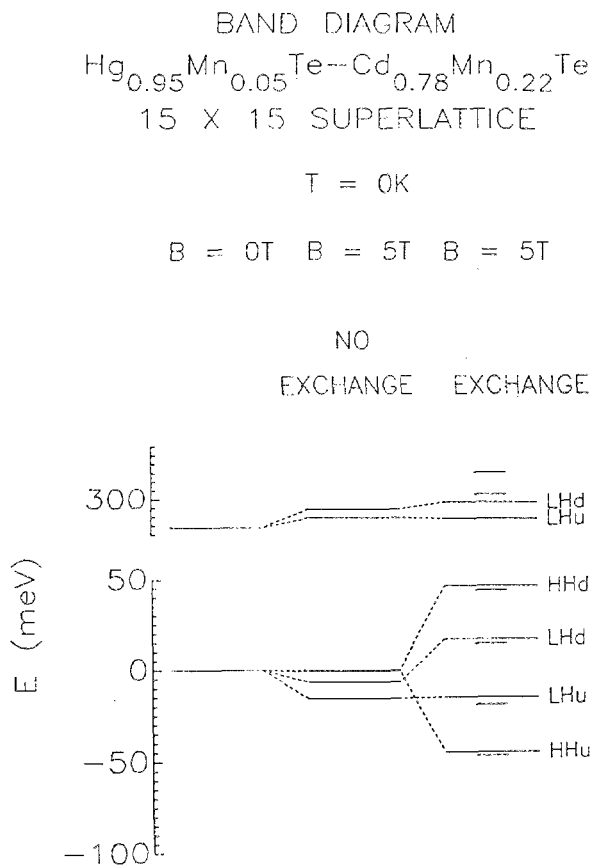


FIG. 4. Energy levels of the lowest conduction-band and highest valence-band states at $Q_z = 0$ for a $\text{Hg}_{0.95}\text{Mn}_{0.05}\text{Te}/\text{Cd}_{0.78}\text{Mn}_{0.22}\text{Te}$ superlattice consisting of 15 molecular layers of each constituent material for three cases: no magnetic field, a magnetic field of 5 T neglecting exchange interaction, and a magnetic field of 5 T including the exchange interaction.

band states are similar to those in $\text{Cd}_{0.8}\text{Mn}_{0.2}\text{Te}/\text{Cd}_{0.7}\text{Mn}_{0.3}\text{Te}$. However, because the band gap here is smaller, the relative change in the band gap is larger and is $\approx 10\%$.

In Fig. 5, we show the change in band gap with magnetic field at three magnetic fields for a $\text{Hg}_{0.95}\text{Mn}_{0.05}\text{Te}/\text{Cd}_{0.78}\text{Mn}_{0.22}\text{Te}$ superlattice consisting of 15 molecular layers of each alloy as a function of inverse temperature.¹⁹ The arrows indicate the zero temperature asymptotes. At low temperatures the Mn^{++} spins align in the direction opposite to the magnetic field leading to a net interaction with the band electrons. At higher temperatures, the Mn^{++} spins are randomized and there is no net exchange interaction with band electrons (within mean-field theory). From the figure, one sees that the strength of the net exchange interactions decreases rapidly with increasing temperature for temperatures above 5 K. Notice the intersection at about 5 K of the two curves for $B = 10$ and 15 T. Below 5 K, because of Mn^{++} spin saturation, the reduction in the band gap resulting from the enhanced spin splitting is about the same at both magnetic fields. However, at $B = 15$ T the Landau level shift is larger and results in a bit smaller net decrease in the band gap. Above 5 K, the spins are not saturated and the larger magnetic field of 15 T gives rise to a larger net spin of

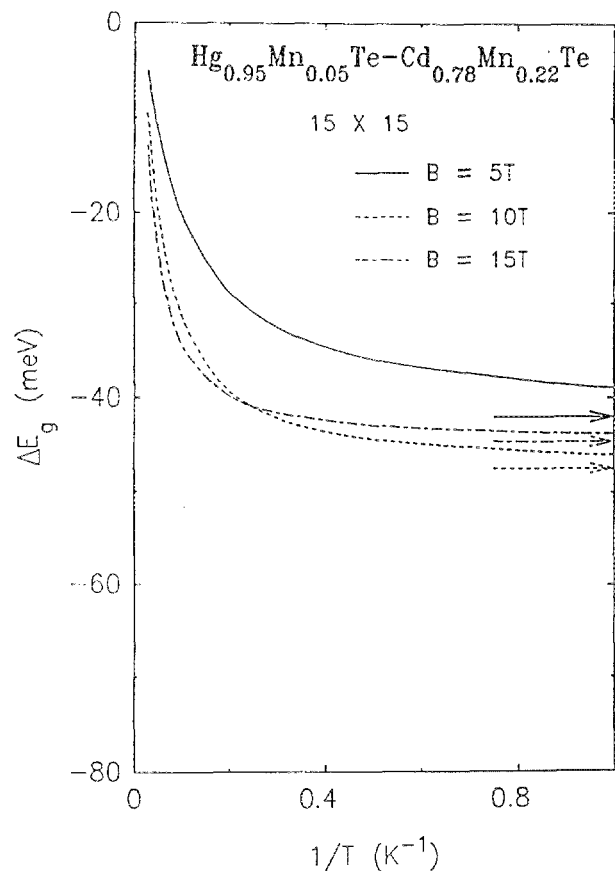


FIG. 5. Change in band gap of the 15×15 $\text{Hg}_{0.95}\text{Mn}_{0.05}\text{Te}/\text{Cd}_{0.78}\text{Mn}_{0.22}\text{Te}$ superlattice as a function of inverse temperature and three magnetic fields. Arrows indicate the zero temperature asymptotes.

Mn^{++} and hence, a larger spin splitting. As a result, the two curves cross each other.

In Fig. 6, we show the change in band gap as a function of valence-band offset at three magnetic fields at zero temperature¹⁹ for a $\text{Hg}_{0.95}\text{Mn}_{0.05}\text{Te}/\text{Cd}_{0.78}\text{Mn}_{0.22}\text{Te}$ superlattice consisting of 15 molecular layers of each alloy. The band gaps are about maximum around zero valence-band offset. As the valence-band offset decreases from zero, both the valence- and conduction-band edges move toward each other. This results in a rapid drop in the band gap. As the valence band offset increases from zero, both band edges move in the same direction but the valence-band edge does faster. This results in a slow decrease in the band gap. The results for $B = 5$ and 10 T are close to each other due to the fact that the spin splittings are about the same at both fields at zero temperature.

In Fig. 7, we show the band gap as a function of magnetic field at zero temperature¹⁹ for a $\text{Hg}_{0.95}\text{Mn}_{0.05}\text{Te}/\text{Cd}_{0.78}\text{Mn}_{0.22}\text{Te}$ superlattice consisting of 15 molecular layers of each alloy for three values of valence-band offset. The curves become flat as we increase the magnetic field, and hence Landau level shift, which opposes reducing the band gap. The derivatives of the band gap with magnetic field at low magnetic field are also shown. At negative valence-band offset, the hole is confined in the $\text{Cd}_{0.78}\text{Mn}_{0.22}\text{Te}$ layer where the exchange interaction is larger. When the valence-band

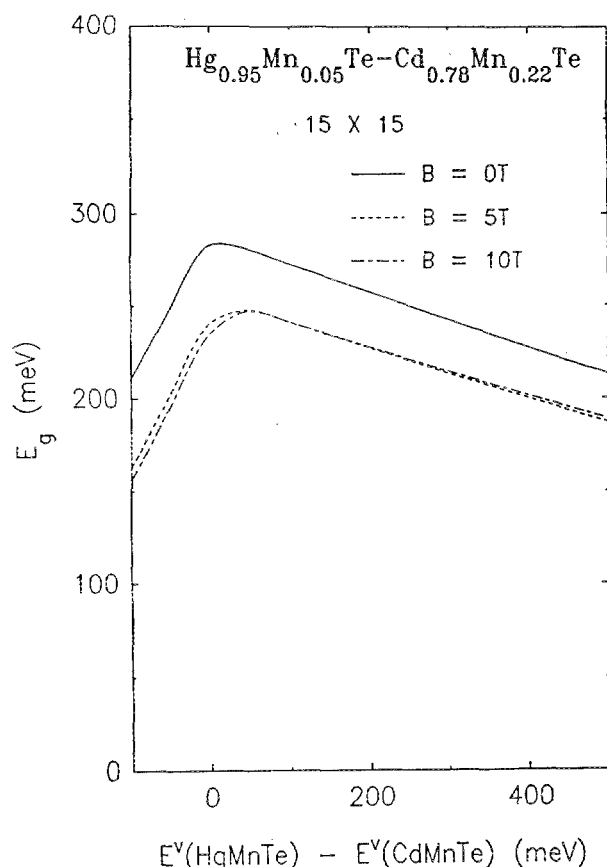


FIG. 6. Band gap of the 15×15 $\text{Hg}_{0.95}\text{Mn}_{0.05}\text{Te}/\text{Cd}_{0.78}\text{Mn}_{0.22}\text{Te}$ superlattice as a function of the valence-band offset at zero temperature for three magnetic fields.

offset becomes positive, the hole is confined in $\text{Hg}_{0.95}\text{Mn}_{0.05}\text{Te}$ where the exchange interaction is smaller. Consequently, the magnitude of the derivative decreases as the valence-band offset increases from negative to positive value.

V. CONCLUSIONS

In summary, we have made our first theoretical study of electronic properties of semimagnetic superlattices. Our theory has used both mean-field theory and virtual-crystal approximation. Therefore, the theory is believed to be as valid as the theory of semimagnetic semiconductor alloys with the same approximations. In the wide-gap system, the value of the valence-band offset is chosen in accordance with the experiments. In the narrow-gap system, values of effective spin and temperature describing antiferromagnetic cluster formation are obtained by linear extrapolation and/or interpolation extracted from the table for CdMnTe . Some uncertainty is expected to be caused by these choices. We have specifically calculated the dependencies of the band gap on the layer thickness, temperature, magnetic field, and valence-band offset for $\text{Hg}_{0.95}\text{Mn}_{0.05}\text{Te}/\text{Cd}_{0.78}\text{Mn}_{0.22}\text{Te}$ and $\text{Cd}_{0.8}\text{Mn}_{0.2}\text{Te}/\text{Cd}_{0.7}\text{Mn}_{0.3}\text{Te}$ superlattices. The exchange interaction is dominant in $\text{Cd}_{0.8}\text{Mn}_{0.2}\text{Te}/\text{Cd}_{0.7}\text{Mn}_{0.3}\text{Te}$ superlattices. But the Landau splitting is also important in $\text{Hg}_{0.95}\text{Mn}_{0.05}\text{Te}/\text{Cd}_{0.78}\text{Mn}_{0.22}\text{Te}$ superlattices. Above 5 K,

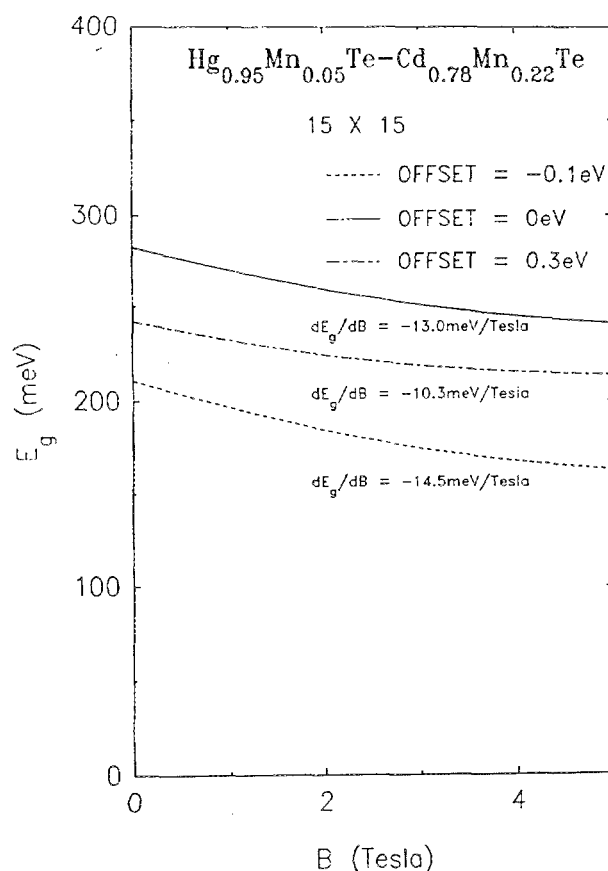


FIG. 7. Band gap of the 15×15 $\text{Hg}_{0.95}\text{Mn}_{0.05}\text{Te}/\text{Cd}_{0.78}\text{Mn}_{0.22}\text{Te}$ superlattice as a function of magnetic field for three valence-band offsets.

the orientations of Mn^{++} spins are randomized, the exchange interaction is small and hence, the band-gap reduction is small. In $\text{Cd}_{0.8}\text{Mn}_{0.2}\text{Te}/\text{Cd}_{0.7}\text{Mn}_{0.3}\text{Te}$ system, the valence-band offset is small. As a result, holes are not strongly confined in the small-band-gap ($X = 0.2$ alloy) material layers and the magnetic properties of the superlattice are similar to that of an alloy. In $\text{Hg}_{0.95}\text{Mn}_{0.05}\text{Te}/\text{Cd}_{0.78}\text{Mn}_{0.22}\text{Te}$ system, the band gap peaks around zero offset. The change in the band gap at low field is found to decrease, with the offset varying from negative to positive value as the site of hole confinement shifts from $\text{Cd}_{0.78}\text{Mn}_{0.22}\text{Te}$ to $\text{Hg}_{0.95}\text{Mn}_{0.05}\text{Te}$ layers. The fraction of change in the band gap is larger in the narrow-gap material ($\approx 10\%$) than that in the wide-gap material ($\approx 2.5\%$) at a low temperature (such as 5 K) and a large magnetic field (such as 5 T).

ACKNOWLEDGMENTS

Two of the authors (G.Y.W. and T.C.M.) would like to acknowledge the support of the Army Research Office under Contract No. DAAG-29-83-K-0104. The work of D.L.S. was supported by Los Alamos National Laboratory Internal Supporting Research.

¹L. A. Kolodziejski, T. Sakamoto, R. L. Gunshor, and S. Datta, *Appl. Phys. Lett.* **44**, 799 (1984).

- ²L. A. Kolodziejski, T. C. Bonsett, R. L. Gunshor, S. Datta, R. B. Bylisma, W. M. Becker, and N. Otsuka, *Appl. Phys. Lett.* **45**, 440 (1984).
- ³R. N. Bicknell, R. Yanka, N. C. Giles-Taylor, D. K. Banks, E. L. Buckland, and J. F. Schetzina, *Appl. Phys. Lett.* **45**, 92 (1984).
- ⁴A. Petrou, J. Warnock, R. N. Bicknell, N. C. Giles-Taylor, and J. F. Schetzina, *Appl. Phys. Lett.* **46**, 692 (1985).
- ⁵J. P. Faurie, J. Reno, S. Sivananthan, I. K. Sou, X. Chu, M. Boukerche, and P. S. Wijewarnasuriya, *J. Vac. Sci. Technol. A* **4**, 2067 (1986).
- ⁶L. A. Kolodziejski, R. L. Gunshor, N. Otsuka, X. C. Zhang, S. K. Chang, and A. V. Nurmikko, *Appl. Phys. Lett.* **47**, 882 (1985).
- ⁷X. C. Zhung, S. K. Chang, A. V. Nurmikko, L. A. Kolodziejski, R. L. Gunshor, and S. Datta, *Phys. Rev. B* **31**, 4056 (1985).
- ⁸X. C. Zhung, S. K. Chang, A. V. Nurmikko, D. Heiman, L. A. Kolodziejski, R. L. Gunshor, and S. Datta, *Solid State Commun.* **56**, 255 (1985).
- ⁹A. V. Nurmikko, X. C. Zhung, S. K. Chang, L. A. Kolodziejski, R. L. Gunshor, and S. Datta, *J. Lumin.* **34**, 89 (1985).
- ¹⁰E. D. Isaacs, D. Heiman, J. J. Zayhowski, R. N. Bicknell, and J. F. Schetzina, *Appl. Phys. Lett.* **48**, 275 (1986).
- ¹¹D. L. Smith and C. Mailhot, *Phys. Rev. B* **33**, 8345 (1986); C. Mailhot and D. L. Smith, *ibid.* **33**, 8360 (1986).
- ¹²M. Jaczynski, J. Kossut, and R. R. Galazka, *Phys. Status Solidi B* **88**, 73 (1978).
- ¹³G. Bastard, C. Rigaux, Y. Guldner, J. Mycielski, and A. Mycielski, *J. Phys. (Paris)* **39**, 87 (1978).
- ¹⁴J. A. Gaj, R. Planel, and G. Fishman, *Solid State Commun.* **29**, 435 (1970).
- ¹⁵I. I. Lyapilin and I. M. Tsivil'kovskii, *Sov. Phys. Usp.* **28**(5), 349 (1985).
In the calculation, we extend the table of effective temperature and spin given by them with a linear interpolation and/or extrapolation extracted from the table for CdMnTe given in Ref. 14.
- ¹⁶P. Lawaetz, *Phys. Rev. B* **10**, 3460 (1971).
- ¹⁷N. B. Brandt and V. V. Moshchalkov, *Adv. Phys.* **33**, 193 (1984).
- ¹⁸J. K. Furdyna, *J. Vac. Sci. Technol. A* **4**, 2002 (1986).
- ¹⁹We neglect the possible formation of a spin glass phase.
- ²⁰M. H. Weiler, R. L. Aggarwal, and B. Lax, *Phys. Rev. B* **17**, 3269 (1978).
- ²¹M. von Ortenberg, *Phys. Rev. Lett.* **49**, 1041 (1982).